Photoinstability of Some Tyrphostin Drugs: Chemical Consequences of Crystallinity

Narendra Kumar,[1,3] Vincent Windisch,[1] and Herman L. Ammon[2]

Received December 8, 1994; accepted August 4, 1995

Purpose. The purpose of this work was to study the photostability of the antiproliferative tyrphostin drug compounds RG 13022(I) and RG 14620(II) as a part of preformulation program.

Methods. The compounds were exposed to cool white fluorescent light in solution as well as in the solid state and analyzed by HPLC. The degradation products were isolated chromatographically and their structures determined by spectroscopic methods. X-ray crystallographic analyses of the above compounds and their solid state degradation products were carried out to understand the mechanism of photodegradation.

Results. The compounds were found to undergo efficient photochemical transformations in solution as well as in the solid state. The degradation in the solution was due to the photoisomerization into their E-isomers (III and IV). The solid state photodegradation products were [2 + 2]-cycloaddition products (V and VI). The stereochemistry of the photocycloaddition products was indicative of the crystal packing of their monomeric precursors. The photocycloaddition product of RG 13022 possesses the head-to-tail linkage as expected from the head-to-tail packing of RG 13022 molecules in the crystal. The photocycloaddition product of RG 14620, however, was found to involve head-to-head linkage in agreement with the head-to-head crystal packing of RG 14620.

Conclusions. Drug compounds containing open chain olefinic double bonds could be sensitive to mild condition of light in the solid state if the distance between the two double bonds in the crystal approaches 4.2°A and they have suitable UV absorption characteristics. Attractive interactions between chlorine atoms have significant influence in controlling the crystal packing of chlorinated aromatic compounds.

KEY WORDS: tyrphostins; photoisomerization; [2 + 2]-cycloaddition; light sensitivity.

INTRODUCTION

Photostability of a drug substance is an important development criterion. Development of a light sensitive compound requires additional protective steps and measures at various stages from synthesis to packaging. For dosage forms likely to receive longer light exposure, such as a dermal ointment, the development of a light sensitive compound could pose some serious challenges. The drug substances RG 13022 (I, Figure 1) and RG 14620 (II, Figure 1) are potent protein tyrosine kinase inhibitors which show potential as antiproliferative agents (1–4) useful in the treatment of psoriasis, a disease in which over signaling via the epidermal growth factor receptor (EGF-R) exists (5–8). This excessive signaling of EGF-R was also demonstrated in human breast cancers (EGF-R and HER-2) and also in atherosclerosis (PDGF-R) (9). RG 14620 also shows efficacy in the tumor growth inhibition in nude mice.

RG 13022(I) and RG 14620(II) are both trisubstituted Z-olefins (Figure 1). During an evaluation of their development potential, stability of I and II in light was studied. The UV spectra of the two compounds are shown in Figure 2. Both these compounds display sensitivity to ambient light (common white cool fluorescent light) in solution. The degradation products are the corresponding (E) isomers (III and IV, Figure 1). To understand the photophysical dynamics responsible for photodegradation, the excited state kinetics of RG 14620 were studied. Rate constants for the photophysical processes and the photochemical quantum yield for RP 14620 were determined. The UV spectra of the (E) isomer IV is shown in figure 2. In the solution state, an equilibrium state between the isomers is achieved at a Z:E ratio of 1:4 under steady state exposure to cool white fluorescent light common in commercial places. RG 13022 and RG 14620 were also sensitive to ambient light in the solid state. RPR 13022 is a pale yellow crystalline solid, m.p. 112°C. When the drug substance was stored open or in clear glass containers in ambient cool white fluorescent light, crumbling of the yellow crystals into a white powdery substance was observed. Analysis of the drug substance by HPLC after exposure to light showed the formation of a major degradation product which was identified as [2 + 2]-cycloaddition product (V, Figure 3). RG 14620, which is a white crystalline solid, m.p. 150°C degraded similarly forming the cycloadduct VI (Figure 3). When the photocycloadducts V and VI were heated at their melting points, the corresponding monomeric olefins I and II were formed respectively.

MATERIALS AND METHODS

RG 13022 and RG 14620 were prepared by Chemical Process Research department at Rhone-Poulenc Rorer. Cis- and trans-Stilbenes were purchased from Aldrich Chemical. UV spectra of the compounds were determined in methanol using a Beckman DU7 spectrophotometer. Degradation in solution as well as in the solid state was followed by HPLC. The HPLC system consisted of a HP 1020 pump, an Applied Biosystems UV detector and a WISP 710 autosampler. The chromatographic separation and analysis of the compounds

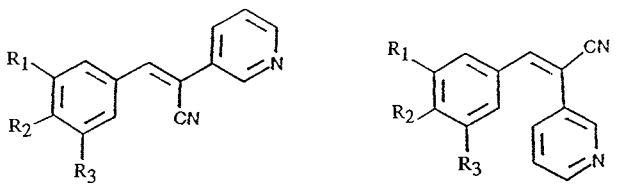

I R_1=R_2= OCH3, R_3=H III R_1=R_2=OCH3, R_3=H
II R_1=R_3=Cl, R_2=H IV R_1=R_3=Cl, R_2=H

Fig. 1. Structure of RG 13022(I), RG 14620(II) and their E-isomers III and IV.

[1] Department of Analytical and Physical Chemistry, Rhone-Poulenc Rorer, Collegeville, Pennsylvania 19426-0107.

[2] Department of Chemistry and Biochemistry, University of Maryland, College Park, Maryland 20742.

[3] To whom correspondence should be addressed.

0724-8741/95/1100-1708$07.50/0

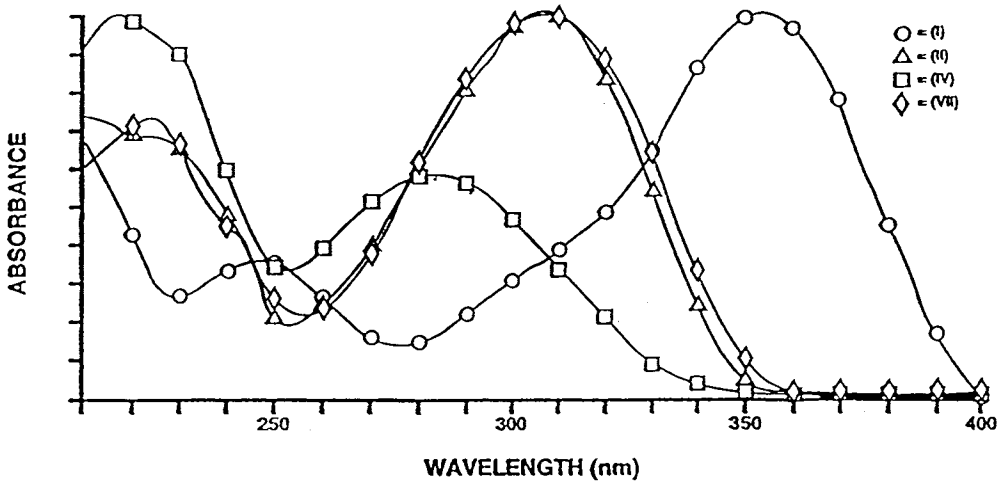

Fig. 2. UV spectra of RG 13022(I), RG 14620(II), the hydrochloride salt (VII) and the E-isomer (IV) of II.

and their degradation products was performed on a C-18, 25 cm × 4.6 mm i.d., 5 μm particle size (Phenomenex) column using 0.05 M ammonium phosphate:acetonitrile (1:1, v/v) as the mobile phase in an isocratic mode at flow rates ranging from 0.8 mL/min. to 1.5 mL/min. The detection was performed by UV absorbance at 254 nm. Quantum yield for the Z to E isomerization of RG 14620 was calculated using trans-stilbene as actinometer. The conversion of trans-stilbene to the cis-isomer was monitored by GC. The GC system consisted of a Varian 4000 chromatograph equipped with a FID detector. Chromatography was performed on a 0.25 mm ID × 30 m, 0.25 μm SPB5 (Supelco) column using Helium at 1 ml/min as the carrier gas. The column temperature was programmed from 100°C to 280°C at 5°C/min. where it was held for 10 min. The injector and FID temperatures were 250°C and 280°C respectively. All X-ray intensity data were collected on an Enraf-Nonius diffractometer with Cu radiation (incident beam monochromator, CuKα, λ = 1.5418°A at 293 K. Cell parameters were obtained from 25 carefully centered reflections. Intensity data were measured with the $2\theta - \theta$ scan procedure at variable scan speeds. The scan range was $\theta = 1.5(w + 0.14 \tan\theta)$, where w is the inherent reflection peak width. Each scan was recorded in 96 steps, with the two outermost 16 step blocks for background determination. 6–8 intensity standards were measured at 1 hr intervals of X-ray exposure. Data for empirical absorption corrections were obtained from ψ-scan measurements of 4–6 reflections. All crystallographic calculations were performed on a DEC Vaxstation II with the TEXSAN (10) program system. The structures were solved with the MITHRIL (11) direct methods sub-program of TEXSAN. Structure refinement was with full matrix least squares. With the exception of RG 14620, hydrogen atoms were refined with individual isotrophic temperature factors; the RG 14620 hydrogen positions were fixed at positions determined by the heavy atom geometries. The calculations included corrections for variation of the intensity standards, empirical absorption and secondary extinction.

The crystallographic data are summarized in Table I. Table II–V give bond lengths and angles. The numbers in parentheses are estimated standard deviations. Temperature factor units are °A; $B_{eq} = (8\pi^2) \Sigma U_{ij} a_i a_j a_i \cdot a_j$. PLOTMD program (12) was used to display the ORTEP drawings (13)

V

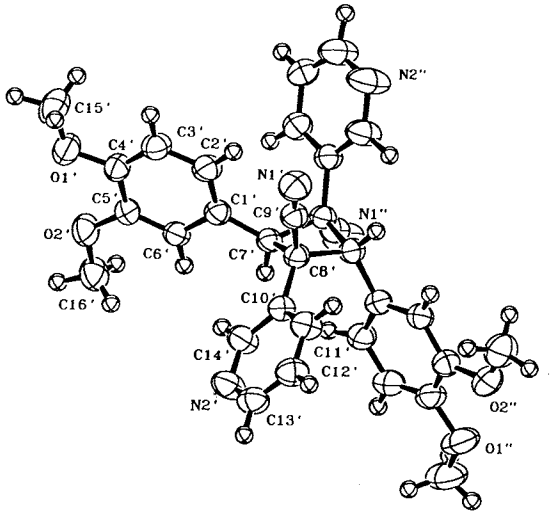

VI

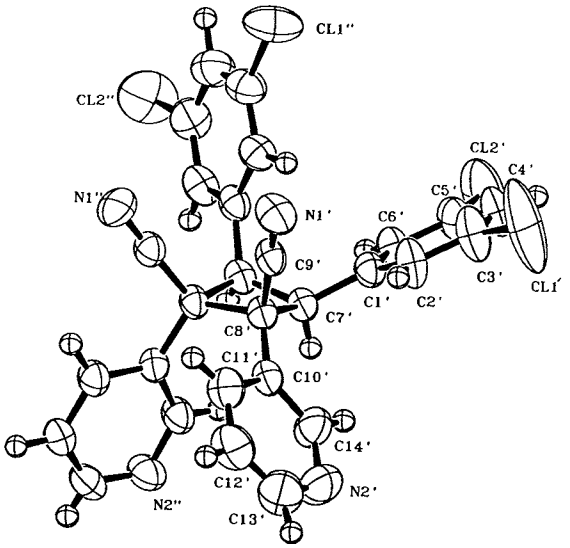

Fig. 3. ORTEP diagrams of the [2 + 2]-photocycloadducts V and VI.

Table I. Crystallographic Data for Compounds I, II, V and VI

	I	II	V	VI
Molecular formula	$C_{16}H_{14}N_2O_4$	$C_{14}H_8N_2Cl_2$	$C_{32}H_{28}N_4O_4$	$C_{28}H_{16}N_4Cl_4$
Formula weight	266.3	275.1	532.60	550.3
Crystal dimensions	irregular shape, 0.3 × 0.4 × 0.5 mm	bent rod. 0.06 × 0.08 × 0.33 mm	flat parallelgram, 0.08 × 0.16 mm × 0.35 mm	flat, distorted hexagon, 0.1 × 0.2 × 0.5 mm
Crystal system	orthorhombic	orthorhombic	triclinic	monoclinic
Lattice parameters:				
a =	26.04 (1) Å	19.696 (5) Å	10.686 (1) Å	17.536 (1) Å
b =	13.360 (7) Å	16.018 (3) Å	11.0455 (6) Å	6.6970 (9) Å
c =	8.008 (2) Å	3.9535 (7) Å	12.951 (1) Å	22.330 (1) Å
α =			90.36 (6) °	
β =			109.28 (8) °	96.525 (5) °
γ =			105.89 (6) °	
Unit cell volume	2786 (5) $Å^3$	1247 (2) $Å^3$	1379.9 (5) $Å^3$	2605.3 (7) $Å^3$
Space group	Pbca (#61)	$Pna2_1$ (#33)	P-1 (#2)	P $2_1/c$ (#14)
Z value	8	4	2	4
ρcalc	1.27 g cm^{-3}	1.46 g cm^{-3}	1.28 g cm^{-3}	1.40 g cm^{-3}
F(000)	1128 e	244 e	560 e	1120 e
μ	7.0 cm^{-1}	46.0 cm^{-1}	7.1 cm^{-1}	43.3 cm^{-1}
Maximum 2θ	120.0°	119.4°	119.9°	140.2°
# Std reflections; I variation; average I variation	6; −1.5 to 2.3%; 0.3%	8; −1.1 to 0.8% −0.1%	7; −23.7 to 0.9; −10.3%	8; −7.8 to −0.2%; −4.8%
Data summary:				
# total data measured	2885	4245	4457	5789
# data without standards	2807	3893	4338	5537
# unique data	2395	1179	4100	5394
# data with I >3σ(I)	1585	764	3327	3698
R_{sym}	0.010 for 2 × 412 data	0.05 for 2 × 388, 4 × 742, 5 × 25 data	0.017 for 2 × 232, 3 × 3 data	0.004 for 2 × 143 data
Ψ-scan transmission factor range	0.877–1.0, av. 0.895	0.769–1.0, av. 0.876	0.944–1.0; av. 0.979	0.879–1.0, av. 0.703
Number of variables	238	170	474	390
R factors: R; R_{wtd}	0.051; 0.091	0.057; 0.074	0.049; 0.088	0.062; 0.089
Goodness of fit indicator	2.47	1.33	2.48	2.04
Maximum shift in final least-squares cycle	0.49	0.18	0.30	0.21
Min, max peaks in final ΔF map	−0.31, 0.24 e $Å^{-3}$	−0.36, 0.39 e $Å^{-3}$	−0.19, 0.22 e $Å^{-3}$	−0.58, 0.78 e $Å^{-3}$

on the VaxStation monitor, introduce atoms labels and prepare plot files for a Hewlett-Packard LaserjetII printer.

RESULTS AND DISCUSSION

The tyrphostins I and II contain olefinic bonds. Both these compounds degraded in the solution state. The degradation reaction was identified as cis-trans geometrical isomerization induced by light. The solutions stored in the dark were stable. This photoreaction produces excited molecular singlet state (S_1) or lowest triplet state (T_1) as likely candidates for the initiation of reaction. The S_1 or T_1 state produced then undergoes a twisting motion about the C=C double bond until a critical twisted geometry is reached and rapid conversion to the ground state (So) occurs. The efficiency of the photoisomerization is described by the quantum yield of the process along with other excited state kinetic data listed in table VI. Solutions of the E-isomers protected from light did not show any conversion into Z-isomer but on exposure to light they isomerized back into their respective Z-isomers. An equilibrium is achieved between the Z and E isomers which favors the latter when exposed to cool white fluorescent light. The Equilibrium Z:E ratios for I and II were observed to be 1:4 by HPLC analysis of an equilibrated solution correcting for the difference in the UV response factors at 254 nm which was used as the detection wavelength. This photostationary ratio did not show any significant change in common organic solvents but would be a function of excitation wavelength(s). The compounds I and II were both crystalline and showed instability when stored under ambient light conditions. Each produced one major degradation product which was different from the solution state degradation products III and IV. The degradation products were identified as cyclobutane dimers V and VI respectively by spectroscopic methods and their structures confirmed by single crystal X-ray analysis. ORTEP diagrams of V and VI are shown in figure 3. This solid state degradation results from the [2 + 2]-cycloaddition reaction induced by room light (cool white fluorescent) in which the intermolecular photodimerization between the two reacting molecules results in the formation of 2 new sigma bonds and a cyclobutane ring. The photoreaction proceeded with stereochemical control and provided predominantly one product in each case. The [2 + 2]-photocyclodimer (V) of I has the trans

Table II. Bond Lengths and Angles for I

atoms		distance	atoms		distance
O1	C4	1.359 (4)	C3	C4	1.380 (5)
O1	C15	1.428 (5)	C4	C5	1.402 (5)
02	C5	1.365 (4)	C5	C6	1.368 (4)
O2	C16	1.428 (5)	C7	C8	1.348 (5)
N1	C9	1.144 (4)	C8	C9	1.448 (5)
N2	C13	1.325 (6)	C8	C10	1.473 (5)
N2	C14	1.337 (5)	C10	C11	1.378 (5)
C1	C2	1.388 (5)	C10	C14	1.381 (5)
C1	C6	1.401 (5)	C11	C12	1.381 (5)
C1	C7	1.451 (5)	C12	C13	1.360 (6)
C2	C3	1.382 (5)			

atoms			angle	atoms			angle
C4	O1	C15	117.8 (3)	C1	C6	C5	121.3 (3)
C5	O2	C16	117.3 (3)	C1	C7	C8	132.5 (3)
C13	N2	C14	117.5 (4)	C7	C8	C9	121.4 (3)
C2	C1	C6	117.7 (3)	C7	C8	C10	123.8 (3)
C2	C1	C7	117.4 (3)	C9	C8	C10	114.8 (3)
C6	C1	C7	125.0 (3)	N1	C9	C8	177.5 (4)
C1	C2	C3	121.6 (3)	C8	C10	C11	121.4 (3)
C2	C3	C4	120.0 (3)	C8	C10	C14	122.0 (3)
O1	C4	C3	125.5 (3)	C11	C10	C14	116.6 (3)
O1	C4	C5	115.2 (3)	C10	C11	C12	120.0 (4)
C3	C4	C5	119.2 (3)	C11	C12	C13	118.5 (4)
O2	C5	C4	114.8 (3)	N2	C13	C12	123.2 (4)
O2	C5	C6	125.1 (3)	N2	C14	C10	123.9 (4)
C4	C5	C6	120.1 (3)				

head-to-tail geometry and is a mirror symmetry product. The crystal packing diagram shown in figure 4 shows that the two adjacent molecules are oriented in a head-to-tail manner and are related by a center of symmetry. The geometry of the [2 + 2]-photocycloadduct (VI) derived from RG 14620(II) is different. In this case the cyclobutane product formed has the trans but head-to-head orientation. The photocyclodimer VI is an inversion symmetry product. The packing diagram

Table III. Bond Lengths and Angles for II

atoms		distance	atoms		distance
CL1	C3	1.73 (1)	C4	C5	1.37 (1)
CL2	C5	1.752 (9)	C5	C6	1.37 (1)
N1	C9	1.14 (1)	C7	C8	1.35 (1)
N2	C13	1.34 (1)	C8	C9	1.41 (1)
N2	C14	1.33 (1)	C8	C10	1.49 (1)
C1	C2	1.39 (1)	C10	C11	1.37 (1)
C1	C6	1.39 (1)	C10	C14	1.39 (1)
C1	C7	1.47 (1)	C11	C12	1.39 (1)
C2	C3	1.39 (1)	C12	C13	1.35 (1)
C3	C4	1.37 (1)			

atoms			angle	atoms		atom	angle
C13	N2	C14	116.1 (9)	C1	C7	C8	131.9 (8)
C2	C1	C6	118.7 (8)	C7	C8	C9	121.4 (8)
C2	C1	C7	116.4 (8)	C7	C8	C10	121.9 (8)
C6	C1	C7	124.8 (8)	C9	C8	C10	116.7 (8)
C1	C2	C3	120.3 (9)	N1	C9	C8	178 (1)
CL1	C3	C2	117.9 (8)	C8	C10	C11	120.9 (8)
CL1	C3	C4	120.6 (7)	C8	C10	C14	121.6 (8)
C2	C3	C4	121.5 (9)	C11	C10	C14	117.5 (8)
C3	C4	C5	117.2 (9)	C10	C11	C12	119.0 (9)
CL2	C5	C4	117.6 (8)	C11	C12	C13	118.9 (9)
CL2	C5	C6	119.0 (7)	N2	C13	C12	123.9 (9)
C4	C5	C6	123.4 (9)	N2	C14	C10	124.5 (9)
C1	C6	C5	119.0 (8)				

Table IV. Bond Lengths and Angles for V

atoms		distance	atoms		distance
O1′	C4′	1.364 (4)	C12′	C13′	1.372 (5)
O1′	C15′	1.406 (5)	O1″	C4″	1.363 (4)
O2′	C5′	1.363 (4)	O1″	C15″	1.414 (6)
O2′	C16′	1.421 (4)	O2″	C5″	1.369 (4)
N1′	C9′	1.138 (4)	O2″	C16″	1.413 (5)
N2′	C13′	1.319 (4)	N1″	C9″	1.140 (4)
N2′	C14′	1.342 (4)	N2″	C13″	1.326 (5)
C1′	C2′	1.389 (4)	N2″	C14″	1.344 (4)
C1′	C6′	1.400 (4)	C1″	C2″	1.373 (4)
C1′	C7′	1.503 (4)	C1″	C6″	1.391 (4)
C2′	C3′	1.390 (5)	C1″	C7″	1.519 (4)
C3′	C4′	1.372 (4)	C2″	C3″	1.403 (5)
C4′	C5′	1.400 (4)	C3″	C4″	1.378 (5)
C5′	C6′	1.378 (4)	C4″	C5″	1.401 (5)
C7′	C8′	1.558 (4)	C5″	C6″	1.379 (4)
C7′	C8″	1.585 (4)	C7″	C8″	1.571 (4)
C8′	C9′	1.468 (4)	C8″	C9″	1.464 (4)
C8′	C10′	1.525 (4)	C8″	C10″	1.539 (4)
C8′	C7″	1.590 (4)	C10″	C11″	1.388 (4)
C10′	C11′	1.379 (4)	C10″	C14″	1.364 (4)
C10′	C14′	1.377 (4)	C11″	C12″	1.377 (5)
C11′	C12′	1.372 (5)	C12″	C13″	1.355 (5)

atoms			angle	atoms			angle
C4′	O1′	C15′	116.9 (3)	C8′	C10′	C14′	122.6 (3)
C5′	O2′	C16′	117.7 (3)	C11′	C10′	C14′	116.9 (3)
C13′	N2′	C14′	116.6 (3)	C10′	C11′	C12′	119.9 (3)
C2′	C1′	C6′	118.7 (3)	C11′	C12′	C13′	118.3 (3)
C2′	C1′	C7′	123.2 (3)	N2′	C13′	C12′	123.9 (3)
C6′	C1′	C7′	118.0 (3)	N2′	C14′	C10′	124.4 (3)
C1′	C2′	C3′	120.0 (3)	C4″	O1″	C15″	117.6 (3)
C2′	C3′	C4′	121.2 (3)	C5″	O2″	C16″	116.9 (3)
O1′	C4′	C3′	125.0 (3)	C13″	N2″	C14″	117.2 (3)
O1′	C4′	C5′	115.7 (3)	C2″	C1″	C6″	119.3 (3)
C3′	C4′	C5′	119.3 (3)	C2″	C1″	C7″	125.0 (3)
O2′	C5′	C4′	114.9 (3)	C6″	C1″	C7″	115.6 (3)
O2′	C5′	C6′	125.3 (3)	C1″	C2″	C3″	120.0 (3)
C4′	C5′	C6′	119.7 (3)	C2″	C3″	C4″	120.6 (3)
C1′	C6′	C5′	121.0 (3)	O1″	C4″	C3″	124.7 (3)
C1′	C7′	C8′	122.2 (3)	O1″	C4″	C5″	116.1 (3)
C1′	C7′	C8″	125.5 (2)	C3″	C4″	C5″	119.2 (3)
C8′	C7′	C8″	88.9 (2)	O2″	C5″	C4″	115.4 (3)
C7′	C8′	C9′	114.6 (2)	O.2″	C5″	C6″	125.0 (3)
C7′	C8′	C10′	117.6 (2)	C4″	C5″	C6″	119.6 (3)
C7′	C8′	C7″	88.5 (2)	C1″	C6″	C5″	121.2 (3)
C9′	C8′	C10′	107.6 (2)	C8′	C7″	C1″	115.3 (2)
C9′	C8′	C7″	108.4 (2)	C8′	C7″	C8″	88.3 (2)
C10′	C8′	C7″	119.3 (2)	C1″	C7″	C8″	120.8 (2)
N1′	C9′	C8′	176.0 (3)	C7′	C8″	C7″	88.2 (2)
C8′	C10′	C11′	120.5 (3)	C7′	C8″	C9″	113.6 (2)
C7′	C8″	C10″	115.0 (2)				
C7″	C8″	C9″	116.8 (2)				
C7″	C8″	C10″	116.5 (2)				
C9″	C8″	C10″	106.3 (2)				
N1″	C9″	C8″	176.9 (3)				
C8″	C10″	C11″	118.3 (3)				
C8″	C10″	C14″	123.8 (3)				
C11″	C10″	C14″	117.8 (3)				
C10″	C11″	C12″	119.1 (3)				
C11″	C12″	C13″	118.6 (3)				
N2″	C13″	C12″	123.8 (3)				
N2″	C14″	C10″	123.4 (3)				

Table V. Bond Lengths and Angles for VI

atoms		distance	atoms		distance
CL1′	C3′	1.727 (4)	C12′	C13′	1.365 (7)
CL2′	C5′	1.732 (4)	CL1″	C3″	1.733 (4)
N1′	C9′	1.138 (4)	CL2″	C5″	1.727 (4)
N2′	C13′	1.319 (6)	N1″	C9″	1.136 (4)
N2′	C14′	1.345 (5)	N2″	C13″	1.330 (5)
C1′	C2′	1.380 (5)	N2″	C14″	1.327 (4)
C1′	C6′	1.382 (5)	C1″	C2″	1.397 (5)
C1′	C7′	1.508 (4)	C1″	C6″	1.384 (5)
C2′	C3′	1.377 (5)	C1″	C7″	1.507 (5)
C3′	C4′	1.354 (6)	C2″	C3″	1.381 (5)
C4′	C5′	1.361 (6)	C3″	C4″	1.370 (6)
C5′	C6′	1.376 (5)	C4″	C5″	1.371 (6)
C7′	C8′	1.563 (4)	C5″	C6″	1.377 (6)
C7′	C7″	1.558 (5)	C7″	C8″	1.585 (4)
C8′	C9′	1.468 (4)	C8″	C9″	1.472 (4)
C8′	C10′	1.511 (5)	C8″	C10″	1.518 (4)
C8′	C8″	1.628 (4)	C10″	C11″	1.384 (4)
C10′	C11′	1.394 (5)	C10″	C14″	1.392 (5)
C10′	C14′	1.370 (5)	C11″	C12″	1.373 (5)
C11′	C12′	1.359 (6)	C12″	C13″	1.364 (6)

atoms			angle	atoms			angle
C13′	N2′	C14′	116.4 (4)	C10′	C11′	C12′	119.2 (4)
C2′	C1′	C6′	118.7 (3)	C11′	C12′	C13′	119.2 (4)
C2′	C1′	C7′	122.7 (3)	N2′	C13′	C12′	123.9 (5)
C6′	C1′	C7′	118.4 (3)	N2′	C14′	C10′	124.4 (4)
C1′	C2′	C3′	119.4 (4)	C13″	N2″	C14″	116.6 (3)
CL1′	C3′	C2′	119.4 (4)	C2″	C1″	C6″	119.0 (3)
CL1′	C3′	C4′	118.2 (3)	C2″	C1″	C7″	122.5 (3)
C2′	C3′	C4′	122.4 (4)	C6″	C1″	C7″	118.4 (3)
C3′	C4′	C5′	117.8 (4)	C1″	C2″	C3″	119.2 (4)
CL2′	C5′	C4′	118.9 (3)	CL1″	C3″	C2″	118.9 (3)
CL2′	C5′	C6′	119.1 (3)	CL1″	C3″	C4″	119.1 (3)
C4′	C5′	C6′	121.9 (4)	C2″	C3″	C4″	122.0 (4)
C1′	C6′	C5′	119.8 (4)	C3″	C4″	C5″	118.0 (4)
C1′	C7′	C8′	123.0 (3)	CL2″	C5″	C4″	118.7 (3)
C1′	C7′	C7″	121.3 (3)	CL2″	C5″	C6″	119.3 (3)
C8′	C7′	C7″	92.1 (2)	C4″	C5″	C6″	122.0 (4)
C7′	C8′	C9′	113.5 (2)	C1″	C6″	C5″	119.7 (4)
C7′	C8′	C10′	119.7 (3)	C7′	C7″	C1″	121.1 (3)
C7′	C8′	C8″	87.2 (2)	C7′	C7″	C8″	89.0 (2)
C9′	C8′	C10′	107.9 (3)	C1″	C7″	C8″	115.5 (3)
C9′	C8′	C8″	109.8 (3)	C8′	C8″	C7″	88.7 (2)
C10′	C8′	C8″	117.4 (2)	C8′	C8″	C9″	112.9 (3)
N1′	C9′	C8′	177.8 (3)	C8′	C8″	C10″	113.7 (3)
C8′	C10′	C11′	120.3 (3)	C7″	C8″	C9″	113.9 (3)
C8′	C10′	C14′	122.7 (3)	C7″	C8″	C10″	116.1 (3)
C11′	C10′	C14′	117.0 (4)	C9″	C8″	C10″	110.1 (2)
N1″	C9″	C8″	177.9 (4)				
C8″	C10″	C11″	122.0 (3)				
C8″	C10″	C14″	121.0 (3)				
C11″	C10″	C14″	117.0 (3)				
C10″	C11″	C12″	119.1 (3)				
C11″	C12″	C13″	119.0 (3)				
N2″	C13″	C12″	123.9 (4)				
N2″	C14″	C10″	124.4 (3)				

of II (Figure 5) shows that the two molecules are related by a mirror plane. The crystallographic data for the monomers RG 13022(I), RG 14620(II) and their corresponding photodimers are given in table I. The stereochemistry of the photodimers and the single crystal X-ray structures of their respective parent compounds show that the photoreaction involves direct bonding of the facing olefinic carbon atoms in their crystal lattices as opposed to the "cross bonding." These products can be formed by photoexcitation of one of the molecule to the π, π^* and concerted addition to the

Table VI. The Excited State Kinetics of the Photoisomerization of RP 14620

Radiative rate constant	k(rad)	$6.7 \times 10^8\ s^{-1}$
Barrier crossing	k(T)	$\gg 10^9\ s^{-1}$
Internal conversion rate	k(IC)	$\sim 10^{12}\ s^{-1}$
Photochemical Quantum yield	Φ	0.46
Branching ratio	α	0.46

neighbouring molecule in the ground state. These results are reminiscent of the pioneering work by Schmidt on cinnamic acids (14). Of the three crystalline forms α, β and γ of cinnamic acid, only α and β-forms react to give dimers upon irradiation in the solid state, the λ form is photostable. The α acid produced inversion symmetry product while the β acid produces mirror symmetry dimer. In both α and β-forms the reactive double bonds in the monomer crystal are closer than a threshhold value of ca. 4.2 °A. In γ crystals the double bond separation is around 4.9°A. The double bond separation in the tyrphostin compounds I and II are below 4.2°A. The E-isomers III and IV were stable in the solid state under ambient light conditions. A distinction in the solution and solid state light instability of these compounds lies in the fact that while the solution state light sensitivity is a molecular property, the solid state photoreactivity is supramolecular in nature and a consequence of their specific crystallinity which facilitates the topochemical photoreaction by providing extraordinary spatial control. This control is not possible in the solution state in which the photodimerization reaction was not observed at least under the ambient light conditions employed above. The two photocyclodimers were stable in ambient room light but underwent thermal [4 → 2 + 2] retrocycloaddition to produce the corresponding monomeric olefins as the dominant products.

The difference in the head-to-tail and head-to-head crystal packing in RG 13022 and RG 14620 which differ only in the nature of phenyl ring substituents deserves some comments. In the absence of hydrogen bonding functionalities the crystal structure of RG 13022(I) can be expected to be controlled by van der Waals forces, geometrical model, size, shape and the surface contours. The crystals of RG 14620(II) are engineered by the chlorine-chlorine attractive interactions (15). This Cl-Cl attractive interaction has been exploited in crystal engineering and to provide a steering device in topochemical reactions (16–18). RG 14620 belongs to the majority class of chlorinated aromatic compounds which follow chloro-rule by showing a crystal packing dominated by chlorine-chlorine interactions.

Understanding of the mechanism of solid state light sensitivity on the basis of the solid state structure suggested that a change in the crystal packing of RG 14620 would have the potential to eliminate solid state light sensitivity. Preparation of quarternary salts of olefinic compounds containing basic moeities has been used to engineer crystals in head-to-tail and head-to-head geometries to produce the desired photocycloadducts (19). Elimination of the solid state photoreactivity of I and II would require a change in the crystal packing which increases the distance between the olefinic double bonds beyond the bonding distance. Preparation of the hydrochloride salt of RG 14620 provided a suitable crystalline

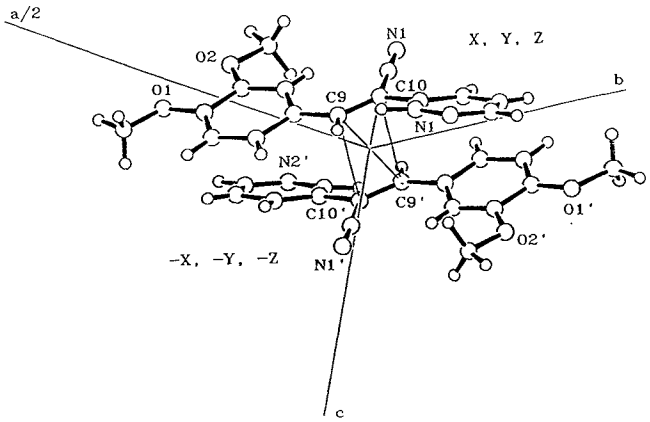

The stereographic packing diagram showing head-to-tail close packing between molecules in the crystal. The space group is Pbca. The indicated distances are C9. . .C10' = 3.906° A, C9. . .C9' = 4.192 °A and C10. . . C10' = 4.071°A.

Fig. 4. Crystal packing diagram of RG 13022(I).

form of the drug substance which was stable in light in the solid state. A single crystal X-ray structure of the salt could not be determined. The solution UV spectrum of the hydrochloride salt (VII, Figure 2) of II is comparable with that of the free base II. It is possible that the crystal structure of the hydrochloride salt is responsible for eliminating the undesirable photosensitivity.

CONCLUSIONS

Compounds containing an olefinic double bond have the potential to show photochemical degradation in solution involving cis-trans isomerization. The relative stability of the cis or trans isomer depends upon their UV/visible absorption characteristics. These compounds can also show instability in the solid state by photochemical mechanisms if, in their crystal structures, the distance between the two double bonds approaches 4°A. Topochemical solid state light sensitivity of a compound can be eliminated by altering the crystal engineering. Salt formation provides a convenient way to achieve this. The crystal engineering of compounds which

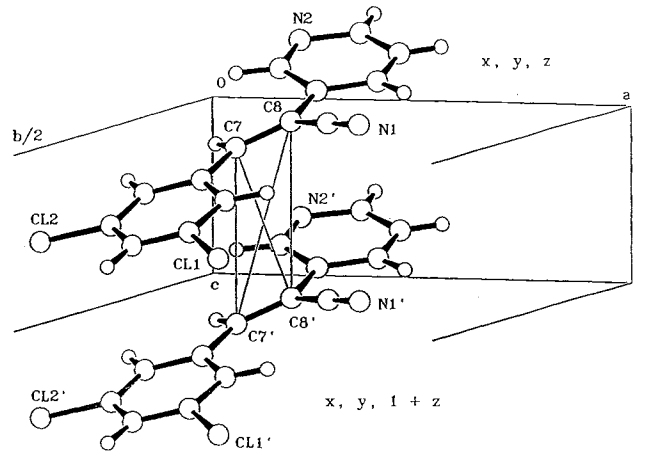

The stereographic packing diagram showing the head-to-head close packing between molecules in the crystal. The space group is $Pna2_1$. The indicated distances C7. . . C7' = C8. . . C8' are 3.953°A, the length of the c-axis, and C7. . . C8' = 3.590 °A.

Fig. 5. Crystal packing diagram of RG 14620(II).

contain chlorinated aromatic moeities in their structures show control by chlorine-chlorine attractive interactions.

ACKNOWLEDGMENTS

Authors are thankful to Dr. A. Spada, Dr. A. Zilberstein and E. Orton and for helpful discussions and Chemical Process Research Department, Rhone-Poulenc Rorer, Collegeville for the material used in this study.

REFERENCES

1. A. Levitzki. Tyrphostins-Potential antiproliferative agents and novel molecular tools, Biochem. Pharmacology. 40:5:913–918 (1990).
2. T. Hunter and J. A. Cooper. Protein Tyrosine kinases, Annual Rev. Biochem. 54:897–930 (1985).
3. G. D. Plowman, A. Ullrich and L. K. Shawver. Receptor tyrosine kinases as targets for drug intervention. DN & P, 7, 6 (1994).
4. A. Levitzki and A. Gazit. Tyrosine kinase inhibition: An approach for the development of many drugs, Science. in press: (1994).
5. J. J. Elder, G. J. Fischer, P. B. Lindquist, G. L. Bennett, M. R. Pittelkow, R. Coffey, L. Ellingsworth, R. Derynck and J. J. Vourhees. Overexpression of transforming growth factor alpha in psoriatic epidermis, Science. 243:811–814 (1988).
6. R. M. Lyall, A. Zilberstein, A. Gazit, C. Gilson, A. Levitzki and J. Schlessinger. Tyrphostins inhibit epidermal growth factor (EGF)-receptor tyrosine kinase activity in living cells and EGF-stimulated cell proliferation, J. Biol. Chem. 264:14503–14509 (1989).
7. B. Margolis, S. G. Ree, S. Felder, M. Merric, R. Lyall, A. Levitzki, A. Ullrich, a. Zilberstein and J. Schlessinger. EGF induces tyrosine phosphorylation of phospholipase C-II: A potential mechanism of EGF receptor signalling, Cell. 57:1101–1107 (1989).
8. A. Gazit, P. Yaish, C. Gilon, and A. Levitzki. Tyrphostins I: Synthesis and biological activity of protein tyrosine kinase inhibitors, J. Med. Chem. 32:2344–2352 (1989).
9. R. Ross. The pathogenesis of atheroclerosis, New Eng. J. of Medicine. 314:488–500 (1986).
10. Molecular Structure Corp. (1965). TEXSAN, Structure Analysis package, ver. 2.0, 3200A Research Forest Drive, The Woodlands, TX 77381 (1987).
11. C. J. Gilmore, MITHRIL. A Computer Program for Automatic Solution of Crystal Structures, University of Glasgow, Glasgow, Scotland, 1983.
12. J. Luo, H. L. Ammon and G. J. Gilliland. PLOTMD, An IOnteractive Program to modify molecular plots on a graphics terminal. J. Appl. Cryst.:22:186 (1989).
13. C. K. Johnson. ORTEP II, Report ORNL-5138. Oakridge National Laboratory, Oak Ridge, TN, (1976).
14. G. M. J. Schmidt. Pure Appl. Chem. 27:647 (1971).
15. G. R. Desiraju. *Organic Solid State Chemistry*, Elsevier, Amsterdam, 1987.
16. B. S. Green and G. M. J. Schmidt. Israel Chemical Society annual meeting abstracts. 190 (1971).
17. B. S. Green and G. M. J. Schmidt. Topochemically-controlled Solid-state Photodimerization to a Tricyclo [6.2.0.$0^{3,6}$] Decane derivative, TetrahedronLetters. 4249 (1970).
18. J. A. R. P. Sarma and G. R. Desiraju. Crystal Engineering via Cl Non bonded interactions. The Novel 2:1 Complex, 6-Chloro3′4,-(methylenedioxy)cinnamic acid. Topochemical conversion into an unsymmetrical cyclobutane and kinetics of the reaction, J. Chem. Soc., Chem. Commu. 145 (1984).
19. F. H. Quina and D. G. Whitten. Medium effects on photochemical reactions. Photochemistry of surfactant Alkyl-4-Stilbazole salts in solution, in the solid state, and in monolayer assemblies, J. Am. Chem. Soc. 97:1602 (1975).